



**University of
Zurich**^{UZH}

**Zurich Open Repository and
Archive**

University of Zurich
University Library
Strickhofstrasse 39
CH-8057 Zurich
www.zora.uzh.ch

Year: 2013

Determination of the X(3872) meson quantum numbers

LHCb Collaboration ; et al ; Bernet, R ; Müller, K ; Steinkamp, O ; Straumann, U ; Vollhardt, A

Abstract: The quantum numbers of the X(3872) meson are determined to be $J^{PC}=1^{++}$ based on angular correlations in $B^+ \rightarrow X(3872)K^+$ decays, where $X(3872) \rightarrow +^- J/\psi$ and $J/\psi \rightarrow +^-$. The data correspond to 1.0 fb⁻¹ of pp collisions collected by the LHCb detector. The only alternative assignment allowed by previous measurements $J^{PC}=2^{--}$ is rejected with a confidence level equivalent to more than 8 Gaussian standard deviations using a likelihood-ratio test in the full angular phase space. This result favors exotic explanations of the X(3872) state.

DOI: <https://doi.org/10.1103/PhysRevLett.110.222001>

Posted at the Zurich Open Repository and Archive, University of Zurich

ZORA URL: <https://doi.org/10.5167/uzh-91818>

Journal Article

Accepted Version

Originally published at:

LHCb Collaboration; et al; Bernet, R; Müller, K; Steinkamp, O; Straumann, U; Vollhardt, A (2013).
Determination of the X(3872) meson quantum numbers. Physical Review Letters, 110(22):222001.

DOI: <https://doi.org/10.1103/PhysRevLett.110.222001>



CERN-PH-EP-2013-017

LHCb-PAPER-2013-001

25 February 2013

Determination of the $X(3872)$ meson quantum numbers

The LHCb collaboration[†]

Abstract

The quantum numbers of the $X(3872)$ meson are determined to be $J^{PC} = 1^{++}$ based on angular correlations in $B^+ \rightarrow X(3872)K^+$ decays, where $X(3872) \rightarrow \pi^+\pi^-J/\psi$ and $J/\psi \rightarrow \mu^+\mu^-$. The data correspond to 1.0 fb^{-1} of pp collisions collected by the LHCb detector. The only alternative assignment allowed by previous measurements, $J^{PC} = 2^{-+}$, is rejected with a confidence level equivalent to more than eight Gaussian standard deviations using the likelihood-ratio test in the full angular phase space. This result favors exotic explanations of the $X(3872)$ state.

Submitted to Physical Review Letters

© CERN on behalf of the LHCb collaboration, license CC-BY-3.0.

[†]Authors are listed on the following pages.

LHCb collaboration

R. Aaij⁴⁰, C. Abellan Beteta^{35,n}, B. Adeva³⁶, M. Adinolfi⁴⁵, C. Adrover⁶, A. Affolder⁵¹,
 Z. Ajaltouni⁵, J. Albrecht⁹, F. Alessio³⁷, M. Alexander⁵⁰, S. Ali⁴⁰, G. Alkhazov²⁹,
 P. Alvarez Cartelle³⁶, A.A. Alves Jr^{24,37}, S. Amato², S. Amerio²¹, Y. Amhis⁷, L. Anderlini^{17,f},
 J. Anderson³⁹, R. Andreassen⁵⁹, R.B. Appleby⁵³, O. Aquines Gutierrez¹⁰, F. Archilli¹⁸,
 A. Artamonov³⁴, M. Artuso⁵⁶, E. Aslanides⁶, G. Auriemma^{24,m}, S. Bachmann¹¹, J.J. Back⁴⁷,
 C. Baesso⁵⁷, V. Balagura³⁰, W. Baldini¹⁶, R.J. Barlow⁵³, C. Barschel³⁷, S. Barsuk⁷,
 W. Barter⁴⁶, Th. Bauer⁴⁰, A. Bay³⁸, J. Beddow⁵⁰, F. Bedeschi²², I. Bediaga¹, S. Belogurov³⁰,
 K. Belous³⁴, I. Belyaev³⁰, E. Ben-Haim⁸, M. Benayoun⁸, G. Bencivenni¹⁸, S. Benson⁴⁹,
 J. Benton⁴⁵, A. Berezhnoy³¹, R. Bernet³⁹, M.-O. Bettler⁴⁶, M. van Beuzekom⁴⁰, A. Bien¹¹,
 S. Bifani¹², T. Bird⁵³, A. Bizzeti^{17,h}, P.M. Bjørnstad⁵³, T. Blake³⁷, F. Blanc³⁸, J. Blouw¹¹,
 S. Blusk⁵⁶, V. Bocci²⁴, A. Bondar³³, N. Bondar²⁹, W. Bonivento¹⁵, S. Borghi⁵³, A. Borgia⁵⁶,
 T.J.V. Bowcock⁵¹, E. Bowen³⁹, C. Bozzi¹⁶, T. Brambach⁹, J. van den Brand⁴¹, J. Bressieux³⁸,
 D. Brett⁵³, M. Britsch¹⁰, T. Britton⁵⁶, N.H. Brook⁴⁵, H. Brown⁵¹, I. Burducea²⁸, A. Bursche³⁹,
 G. Busetto^{21,q}, J. Buytaert³⁷, S. Cadeddu¹⁵, O. Callot⁷, M. Calvi^{20,j}, M. Calvo Gomez^{35,n},
 A. Camboni³⁵, P. Campana^{18,37}, A. Carbone^{14,c}, G. Carboni^{23,k}, R. Cardinale^{19,i}, A. Cardini¹⁵,
 H. Carranza-Mejia⁴⁹, L. Carson⁵², K. Carvalho Akiba², G. Casse⁵¹, M. Cattaneo³⁷, Ch. Cauet⁹,
 M. Charles⁵⁴, Ph. Charpentier³⁷, P. Chen^{3,38}, N. Chiapolini³⁹, M. Chrzasczcz²⁵, K. Ciba³⁷,
 X. Cid Vidal³⁶, G. Ciezarek⁵², P.E.L. Clarke⁴⁹, M. Clemencic³⁷, H.V. Cliff⁴⁶, J. Closier³⁷,
 C. Coca²⁸, V. Coco⁴⁰, J. Cogan⁶, E. Cogneras⁵, P. Collins³⁷, A. Comerma-Montells³⁵,
 A. Contu¹⁵, A. Cook⁴⁵, M. Coombes⁴⁵, S. Coquereau⁸, G. Corti³⁷, B. Couturier³⁷,
 G.A. Cowan³⁸, D. Craik⁴⁷, S. Cunliffe⁵², R. Currie⁴⁹, C. D'Ambrosio³⁷, P. David⁸,
 P.N.Y. David⁴⁰, I. De Bonis⁴, K. De Bruyn⁴⁰, S. De Capua⁵³, M. De Cian³⁹, J.M. De Miranda¹,
 M. De Oyanguren Campos^{35,o}, L. De Paula², W. De Silva⁵⁹, P. De Simone¹⁸, D. Decamp⁴,
 M. Deckenhoff⁹, L. Del Buono⁸, D. Derkach¹⁴, O. Deschamps⁵, F. Dettori⁴¹, A. Di Canto¹¹,
 H. Dijkstra³⁷, M. Dogaru²⁸, S. Donleavy⁵¹, F. Dordei¹¹, A. Dosil Suárez³⁶, D. Dossett⁴⁷,
 A. Dovbnya⁴², F. Dupertuis³⁸, R. Dzhelyadin³⁴, A. Dziurda²⁵, A. Dzyuba²⁹, S. Easo^{48,37},
 U. Egede⁵², V. Egorychev³⁰, S. Eidelman³³, D. van Eijk⁴⁰, S. Eisenhardt⁴⁹, U. Eitschberger⁹,
 R. Ekelhof⁹, L. Eklund⁵⁰, I. El Rifai⁵, Ch. Elsasser³⁹, D. Elsby⁴⁴, A. Falabella^{14,e}, C. Färber¹¹,
 G. Fardell⁴⁹, C. Farinelli⁴⁰, S. Farry¹², V. Fave³⁸, D. Ferguson⁴⁹, V. Fernandez Albor³⁶,
 F. Ferreira Rodrigues¹, M. Ferro-Luzzi³⁷, S. Filippov³², C. Fitzpatrick³⁷, M. Fontana¹⁰,
 F. Fontanelli^{19,i}, R. Forty³⁷, O. Francisco², M. Frank³⁷, C. Frei³⁷, M. Frosini^{17,f}, S. Furcas²⁰,
 E. Furfaro²³, A. Gallas Torreira³⁶, D. Galli^{14,c}, M. Gandelman², P. Gandini⁵⁴, Y. Gao³,
 J. Garofoli⁵⁶, P. Garosi⁵³, J. Garra Tico⁴⁶, L. Garrido³⁵, C. Gaspar³⁷, R. Gauld⁵⁴,
 E. Gersabeck¹¹, M. Gersabeck⁵³, T. Gershon^{47,37}, Ph. Ghez⁴, V. Gibson⁴⁶, V.V. Gligorov³⁷,
 C. Göbel⁵⁷, D. Golubkov³⁰, A. Golutvin^{52,30,37}, A. Gomes², H. Gordon⁵⁴,
 M. Grabalosa Gándara⁵, R. Graciani Diaz³⁵, L.A. Granado Cardoso³⁷, E. Graugés³⁵,
 G. Graziani¹⁷, A. Grecu²⁸, E. Greening⁵⁴, S. Gregson⁴⁶, O. Grünberg⁵⁸, B. Gui⁵⁶,
 E. Gushchin³², Yu. Guz³⁴, T. Gys³⁷, C. Hadjivasiliou⁵⁶, G. Haefeli³⁸, C. Haen³⁷, S.C. Haines⁴⁶,
 S. Hall⁵², T. Hampson⁴⁵, S. Hansmann-Menzemer¹¹, N. Harnew⁵⁴, S.T. Harnew⁴⁵, J. Harrison⁵³,
 T. Hartmann⁵⁸, J. He⁷, V. Heijne⁴⁰, K. Hennessy⁵¹, P. Henrard⁵, J.A. Hernando Morata³⁶,
 E. van Herwijnen³⁷, E. Hicks⁵¹, D. Hill⁵⁴, M. Hoballah⁵, C. Hombach⁵³, P. Hopchev⁴,
 W. Hulsbergen⁴⁰, P. Hunt⁵⁴, T. Huse⁵¹, N. Hussain⁵⁴, D. Hutchcroft⁵¹, D. Hynds⁵⁰,
 V. Iakovenko⁴³, M. Idzik²⁶, P. Ilten¹², R. Jacobsson³⁷, A. Jaeger¹¹, E. Jans⁴⁰, P. Jaton³⁸,
 F. Jing³, M. John⁵⁴, D. Johnson⁵⁴, C.R. Jones⁴⁶, B. Jost³⁷, M. Kabbalo⁹, S. Kandybei⁴²,

M. Karacson³⁷, T.M. Karbach³⁷, I.R. Kenyon⁴⁴, U. Kerzel³⁷, T. Ketel⁴¹, A. Keune³⁸,
B. Khanji²⁰, O. Kochebina⁷, I. Komarov^{38,31}, R.F. Koopman⁴¹, P. Koppenburg⁴⁰, M. Korolev³¹,
A. Kozlinskiy⁴⁰, L. Kravchuk³², K. Kreplin¹¹, M. Kreps⁴⁷, G. Krocker¹¹, P. Krokovny³³,
F. Kruse⁹, M. Kucharczyk^{20,25,j}, V. Kudryavtsev³³, T. Kvaratskheliya^{30,37}, V.N. La Thi³⁸,
D. Lacarrere³⁷, G. Lafferty⁵³, A. Lai¹⁵, D. Lambert⁴⁹, R.W. Lambert⁴¹, E. Lanciotti³⁷,
G. Lanfranchi^{18,37}, C. Langenbruch³⁷, T. Latham⁴⁷, C. Lazzeroni⁴⁴, R. Le Gac⁶,
J. van Leerdam⁴⁰, J.-P. Lees⁴, R. Lefèvre⁵, A. Leflat^{31,37}, J. Lefrançois⁷, S. Leo²², O. Leroy⁶,
B. Leverington¹¹, Y. Li³, L. Li Gioi⁵, M. Liles⁵¹, R. Lindner³⁷, C. Linn¹¹, B. Liu³, G. Liu³⁷,
J. von Loeben²⁰, S. Lohn³⁷, J.H. Lopes², E. Lopez Asamar³⁵, N. Lopez-March³⁸, H. Lu³,
D. Lucchesi^{21,q}, J. Luisier³⁸, H. Luo⁴⁹, F. Machefert⁷, I.V. Machikhiliyan^{4,30}, F. Maciuc²⁸,
O. Maev^{29,37}, S. Malde⁵⁴, G. Manca^{15,d}, G. Mancinelli⁶, U. Marconi¹⁴, R. Märki³⁸, J. Marks¹¹,
G. Martellotti²⁴, A. Martens⁸, L. Martin⁵⁴, A. Martín Sánchez⁷, M. Martinelli⁴⁰,
D. Martinez Santos⁴¹, D. Martins Tostes², A. Massafferri¹, R. Matev³⁷, Z. Mathe³⁷,
C. Matteuzzi²⁰, E. Maurice⁶, A. Mazurov^{16,32,37,e}, J. McCarthy⁴⁴, R. McNulty¹², A. McNab⁵³,
B. Meadows^{59,54}, F. Meier⁹, M. Meissner¹¹, M. Merk⁴⁰, D.A. Milanes⁸, M.-N. Minard⁴,
J. Molina Rodriguez⁵⁷, S. Monteil⁵, D. Moran⁵³, P. Morawski²⁵, M.J. Morello^{22,s},
R. Mountain⁵⁶, I. Mous⁴⁰, F. Muheim⁴⁹, K. Müller³⁹, R. Muresan²⁸, B. Muryn²⁶, B. Muster³⁸,
P. Naik⁴⁵, T. Nakada³⁸, R. Nandakumar⁴⁸, I. Nasteva¹, M. Needham⁴⁹, N. Neufeld³⁷,
A.D. Nguyen³⁸, T.D. Nguyen³⁸, C. Nguyen-Mau^{38,p}, M. Nicol⁷, V. Niess⁵, R. Niet⁹, N. Nikitin³¹,
T. Nikodem¹¹, A. Nomerotski⁵⁴, A. Novoselov³⁴, A. Oblakowska-Mucha²⁶, V. Obraztsov³⁴,
S. Oggero⁴⁰, S. Ogilvy⁵⁰, O. Okhrimenko⁴³, R. Oldeman^{15,d,37}, M. Orlandea²⁸,
J.M. Otalora Goicochea², P. Owen⁵², B.K. Pal⁵⁶, A. Palano^{13,b}, M. Palutan¹⁸, J. Panman³⁷,
A. Papanestis⁴⁸, M. Pappagallo⁵⁰, C. Parkes⁵³, C.J. Parkinson⁵², G. Passaleva¹⁷, G.D. Patel⁵¹,
M. Patel⁵², G.N. Patrick⁴⁸, C. Patrignani^{19,i}, C. Pavel-Nicorescu²⁸, A. Pazos Alvarez³⁶,
A. Pellegrino⁴⁰, G. Penso^{24,l}, M. Pepe Altarelli³⁷, S. Perazzini^{14,c}, D.L. Perego^{20,j},
E. Perez Trigo³⁶, A. Pérez-Calero Yzquierdo³⁵, P. Perret⁵, M. Perrin-Terrin⁶, G. Pessina²⁰,
K. Petridis⁵², A. Petrolini^{19,i}, A. Phan⁵⁶, E. Picatoste Olloqui³⁵, B. Pietrzyk⁴, T. Pilar⁴⁷,
D. Pinci²⁴, S. Playfer⁴⁹, M. Plo Casasus³⁶, F. Polci⁸, G. Polok²⁵, A. Poluektov^{47,33},
E. Polcarpo², D. Popov¹⁰, B. Popovici²⁸, C. Potterat³⁵, A. Powell⁵⁴, J. Prisciandaro³⁸,
V. Pugatch⁴³, A. Puig Navarro³⁸, G. Punzi^{22,r}, W. Qian⁴, J.H. Rademacker⁴⁵,
B. Rakotomiamanana³⁸, M.S. Rangel², I. Raniuk⁴², N. Rauschmayr³⁷, G. Raven⁴¹,
S. Redford⁵⁴, M.M. Reid⁴⁷, A.C. dos Reis¹, S. Ricciardi⁴⁸, A. Richards⁵², K. Rinnert⁵¹,
V. Rives Molina³⁵, D.A. Roa Romero⁵, P. Robbe⁷, E. Rodrigues⁵³, P. Rodriguez Perez³⁶,
S. Roiser³⁷, V. Romanovsky³⁴, A. Romero Vidal³⁶, J. Rouvinet³⁸, T. Ruf³⁷, F. Ruffini²²,
H. Ruiz³⁵, P. Ruiz Valls^{35,o}, G. Sabatino^{24,k}, J.J. Saborido Silva³⁶, N. Sagidova²⁹, P. Sail⁵⁰,
B. Saitta^{15,d}, C. Salzmann³⁹, B. Sanmartin Sedes³⁶, M. Sannino^{19,i}, R. Santacesaria²⁴,
C. Santamarina Rios³⁶, E. Santovetti^{23,k}, M. Sapunov⁶, A. Sarti^{18,l}, C. Satriano^{24,m}, A. Satta²³,
M. Savrie^{16,e}, D. Savrina^{30,31}, P. Schaack⁵², M. Schiller⁴¹, H. Schindler³⁷, M. Schlupp⁹,
M. Schmelling¹⁰, B. Schmidt³⁷, O. Schneider³⁸, A. Schopper³⁷, M.-H. Schune⁷, R. Schwemmer³⁷,
B. Sciascia¹⁸, A. Sciubba²⁴, M. Seco³⁶, A. Semennikov³⁰, K. Senderowska²⁶, I. Sepp⁵²,
N. Serra³⁹, J. Serrano⁶, P. Seyfert¹¹, M. Shapkin³⁴, I. Shapoval^{42,37}, P. Shatalov³⁰,
Y. Shcheglov²⁹, T. Shears^{51,37}, L. Shekhtman³³, O. Shevchenko⁴², V. Shevchenko³⁰, A. Shires⁵²,
R. Silva Coutinho⁴⁷, T. Skwarnicki⁵⁶, N.A. Smith⁵¹, E. Smith^{54,48}, M. Smith⁵³, M.D. Sokoloff⁵⁹,
F.J.P. Soler⁵⁰, F. Soomro^{18,37}, D. Souza⁴⁵, B. Souza De Paula², B. Spaan⁹, A. Sparkes⁴⁹,
P. Spradlin⁵⁰, F. Stagni³⁷, S. Stahl¹¹, O. Steinkamp³⁹, S. Stoica²⁸, S. Stone⁵⁶, B. Storaci³⁹,
M. Straticiuc²⁸, U. Straumann³⁹, V.K. Subbiah³⁷, S. Swientek⁹, V. Syropoulos⁴¹,

M. Szczekowski²⁷, P. Szczypka^{38,37}, T. Szumlak²⁶, S. T’Jampens⁴, M. Teklishyn⁷,
E. Teodorescu²⁸, F. Teubert³⁷, C. Thomas⁵⁴, E. Thomas³⁷, J. van Tilburg¹¹, V. Tisserand⁴,
M. Tobin³⁹, S. Tolk⁴¹, D. Tonelli³⁷, S. Topp-Joergensen⁵⁴, N. Torr⁵⁴, E. Tournefier^{4,52},
S. Tourneur³⁸, M.T. Tran³⁸, M. Tresch³⁹, A. Tsaregorodtsev⁶, P. Tsopelas⁴⁰, N. Tuning⁴⁰,
M. Ubeda Garcia³⁷, A. Ukleja²⁷, D. Urner⁵³, U. Uwer¹¹, V. Vagnoni¹⁴, G. Valenti¹⁴,
R. Vazquez Gomez³⁵, P. Vazquez Regueiro³⁶, S. Vecchi¹⁶, J.J. Velthuis⁴⁵, M. Veltri^{17,g},
G. Veneziano³⁸, M. Vesterinen³⁷, B. Viaud⁷, D. Vieira², X. Vilasis-Cardona^{35,n}, A. Vollhardt³⁹,
D. Volyanskyy¹⁰, D. Voong⁴⁵, A. Vorobyev²⁹, V. Vorobyev³³, C. Voß⁵⁸, H. Voss¹⁰, R. Waldi⁵⁸,
R. Wallace¹², S. Wandernoth¹¹, J. Wang⁵⁶, D.R. Ward⁴⁶, N.K. Watson⁴⁴, A.D. Webber⁵³,
D. Websdale⁵², M. Whitehead⁴⁷, J. Wicht³⁷, J. Wiechczynski²⁵, D. Wiedner¹¹, L. Wiggers⁴⁰,
G. Wilkinson⁵⁴, M.P. Williams^{47,48}, M. Williams⁵⁵, F.F. Wilson⁴⁸, J. Wishahi⁹, M. Witek²⁵,
S.A. Wotton⁴⁶, S. Wright⁴⁶, S. Wu³, K. Wyllie³⁷, Y. Xie^{49,37}, F. Xing⁵⁴, Z. Xing⁵⁶, Z. Yang³,
R. Young⁴⁹, X. Yuan³, O. Yushchenko³⁴, M. Zangoli¹⁴, M. Zavertyaev^{10,a}, F. Zhang³,
L. Zhang⁵⁶, W.C. Zhang¹², Y. Zhang³, A. Zhelezov¹¹, A. Zhokhov³⁰, L. Zhong³, A. Zvyagin³⁷.

¹ Centro Brasileiro de Pesquisas Físicas (CBPF), Rio de Janeiro, Brazil

² Universidade Federal do Rio de Janeiro (UFRJ), Rio de Janeiro, Brazil

³ Center for High Energy Physics, Tsinghua University, Beijing, China

⁴ LAPP, Université de Savoie, CNRS/IN2P3, Annecy-Le-Vieux, France

⁵ Clermont Université, Université Blaise Pascal, CNRS/IN2P3, LPC, Clermont-Ferrand, France

⁶ CPPM, Aix-Marseille Université, CNRS/IN2P3, Marseille, France

⁷ LAL, Université Paris-Sud, CNRS/IN2P3, Orsay, France

⁸ LPNHE, Université Pierre et Marie Curie, Université Paris Diderot, CNRS/IN2P3, Paris, France

⁹ Fakultät Physik, Technische Universität Dortmund, Dortmund, Germany

¹⁰ Max-Planck-Institut für Kernphysik (MPIK), Heidelberg, Germany

¹¹ Physikalisches Institut, Ruprecht-Karls-Universität Heidelberg, Heidelberg, Germany

¹² School of Physics, University College Dublin, Dublin, Ireland

¹³ Sezione INFN di Bari, Bari, Italy

¹⁴ Sezione INFN di Bologna, Bologna, Italy

¹⁵ Sezione INFN di Cagliari, Cagliari, Italy

¹⁶ Sezione INFN di Ferrara, Ferrara, Italy

¹⁷ Sezione INFN di Firenze, Firenze, Italy

¹⁸ Laboratori Nazionali dell’INFN di Frascati, Frascati, Italy

¹⁹ Sezione INFN di Genova, Genova, Italy

²⁰ Sezione INFN di Milano Bicocca, Milano, Italy

²¹ Sezione INFN di Padova, Padova, Italy

²² Sezione INFN di Pisa, Pisa, Italy

²³ Sezione INFN di Roma Tor Vergata, Roma, Italy

²⁴ Sezione INFN di Roma La Sapienza, Roma, Italy

²⁵ Henryk Niewodniczanski Institute of Nuclear Physics Polish Academy of Sciences, Kraków, Poland

²⁶ AGH University of Science and Technology, Kraków, Poland

²⁷ National Center for Nuclear Research (NCBJ), Warsaw, Poland

²⁸ Horia Hulubei National Institute of Physics and Nuclear Engineering, Bucharest-Magurele, Romania

²⁹ Petersburg Nuclear Physics Institute (PNPI), Gatchina, Russia

³⁰ Institute of Theoretical and Experimental Physics (ITEP), Moscow, Russia

³¹ Institute of Nuclear Physics, Moscow State University (SINP MSU), Moscow, Russia

³² Institute for Nuclear Research of the Russian Academy of Sciences (INR RAN), Moscow, Russia

³³ Budker Institute of Nuclear Physics (SB RAS) and Novosibirsk State University, Novosibirsk, Russia

³⁴ Institute for High Energy Physics (IHEP), Protvino, Russia

³⁵ Universitat de Barcelona, Barcelona, Spain

- ³⁶ *Universidad de Santiago de Compostela, Santiago de Compostela, Spain*
³⁷ *European Organization for Nuclear Research (CERN), Geneva, Switzerland*
³⁸ *Ecole Polytechnique Fédérale de Lausanne (EPFL), Lausanne, Switzerland*
³⁹ *Physik-Institut, Universität Zürich, Zürich, Switzerland*
⁴⁰ *Nikhef National Institute for Subatomic Physics, Amsterdam, The Netherlands*
⁴¹ *Nikhef National Institute for Subatomic Physics and VU University Amsterdam, Amsterdam, The Netherlands*
⁴² *NSC Kharkiv Institute of Physics and Technology (NSC KIPT), Kharkiv, Ukraine*
⁴³ *Institute for Nuclear Research of the National Academy of Sciences (KINR), Kyiv, Ukraine*
⁴⁴ *University of Birmingham, Birmingham, United Kingdom*
⁴⁵ *H.H. Wills Physics Laboratory, University of Bristol, Bristol, United Kingdom*
⁴⁶ *Cavendish Laboratory, University of Cambridge, Cambridge, United Kingdom*
⁴⁷ *Department of Physics, University of Warwick, Coventry, United Kingdom*
⁴⁸ *STFC Rutherford Appleton Laboratory, Didcot, United Kingdom*
⁴⁹ *School of Physics and Astronomy, University of Edinburgh, Edinburgh, United Kingdom*
⁵⁰ *School of Physics and Astronomy, University of Glasgow, Glasgow, United Kingdom*
⁵¹ *Oliver Lodge Laboratory, University of Liverpool, Liverpool, United Kingdom*
⁵² *Imperial College London, London, United Kingdom*
⁵³ *School of Physics and Astronomy, University of Manchester, Manchester, United Kingdom*
⁵⁴ *Department of Physics, University of Oxford, Oxford, United Kingdom*
⁵⁵ *Massachusetts Institute of Technology, Cambridge, MA, United States*
⁵⁶ *Syracuse University, Syracuse, NY, United States*
⁵⁷ *Pontifícia Universidade Católica do Rio de Janeiro (PUC-Rio), Rio de Janeiro, Brazil, associated to* ²
⁵⁸ *Institut für Physik, Universität Rostock, Rostock, Germany, associated to* ¹¹
⁵⁹ *University of Cincinnati, Cincinnati, OH, United States, associated to* ⁵⁶

^a *P.N. Lebedev Physical Institute, Russian Academy of Science (LPI RAS), Moscow, Russia*

^b *Università di Bari, Bari, Italy*

^c *Università di Bologna, Bologna, Italy*

^d *Università di Cagliari, Cagliari, Italy*

^e *Università di Ferrara, Ferrara, Italy*

^f *Università di Firenze, Firenze, Italy*

^g *Università di Urbino, Urbino, Italy*

^h *Università di Modena e Reggio Emilia, Modena, Italy*

ⁱ *Università di Genova, Genova, Italy*

^j *Università di Milano Bicocca, Milano, Italy*

^k *Università di Roma Tor Vergata, Roma, Italy*

^l *Università di Roma La Sapienza, Roma, Italy*

^m *Università della Basilicata, Potenza, Italy*

ⁿ *LIFAELS, La Salle, Universitat Ramon Llull, Barcelona, Spain*

^o *IFIC, Universitat de Valencia-CSIC, Valencia, Spain*

^p *Hanoi University of Science, Hanoi, Viet Nam*

^q *Università di Padova, Padova, Italy*

^r *Università di Pisa, Pisa, Italy*

^s *Scuola Normale Superiore, Pisa, Italy*

It has been almost ten years since the narrow $X(3872)$ state was discovered in B^+ decays by the Belle experiment [1].¹ Subsequently, its existence has been confirmed by several other experiments [2–4]. Recently, its production has been studied at the LHC [5, 6]. However, the nature of this state remains unclear. Among the open possibilities are conventional charmonium and exotic states such as $D^{*0}\bar{D}^0$ molecules [7], tetra-quarks [8] or their mixtures [9]. Determination of the quantum numbers, total angular momentum J , parity P , and charge-conjugation C , is important to shed light on this ambiguity. The C -parity of the state is positive since the $X(3872) \rightarrow \gamma J/\psi$ decay has been observed [10, 11].

The CDF experiment analyzed three-dimensional (3D) angular correlations in a relatively high-background sample of 2292 ± 113 inclusively-reconstructed $X(3872) \rightarrow \pi^+\pi^- J/\psi$, $J/\psi \rightarrow \mu^+\mu^-$ decays, dominated by prompt production in $p\bar{p}$ collisions. The unknown polarization of the $X(3872)$ mesons limited the sensitivity of the measurement of J^{PC} [12]. A χ^2 fit of J^{PC} hypotheses to the binned 3D distribution of the J/ψ and $\pi\pi$ helicity angles ($\theta_{J/\psi}$, $\theta_{\pi\pi}$) [13–15], and the angle between their decay planes ($\Delta\phi_{J/\psi, \pi\pi} = \phi_{J/\psi} - \phi_{\pi\pi}$), excluded all spin-parity assignments except for 1^{++} or 2^{-+} . The Belle collaboration observed 173 ± 16 $B \rightarrow X(3872)K$ ($K = K^\pm$ or K_S^0), $X(3872) \rightarrow \pi^+\pi^- J/\psi$, $J/\psi \rightarrow \ell^+\ell^-$ decays [16]. The reconstruction of the full decay chain resulted in a small background and polarized $X(3872)$ mesons, making their helicity angle (θ_X) and orientation of their decay plane (ϕ_X) sensitive to J^{PC} as well. By studying one-dimensional distributions in three different angles, they concluded that their data were equally well described by the 1^{++} and 2^{-+} hypotheses. The BaBar experiment observed 34 ± 7 $X(3872) \rightarrow \omega J/\psi$, $\omega \rightarrow \pi^+\pi^-\pi^0$ events [17]. The observed $\pi^+\pi^-\pi^0$ mass distribution favored the 2^{-+} hypothesis, which had a confidence level (CL) of 68%, over the 1^{++} hypothesis, but the latter was not ruled out (CL = 7%).

In this Letter, we report the first analysis of the complete five-dimensional angular correlations of the $B^+ \rightarrow X(3872)K^+$, $X(3872) \rightarrow \pi^+\pi^- J/\psi$, $J/\psi \rightarrow \mu^+\mu^-$ decay chain using $\sqrt{s} = 7$ TeV pp collision data corresponding to 1.0 fb^{-1} collected in 2011 by the LHCb experiment. The LHCb detector [18] is a single-arm forward spectrometer covering the pseudorapidity range $2 < \eta < 5$, designed for the study of particles containing b or c quarks. The detector includes a high precision tracking system consisting of a silicon-strip vertex detector surrounding the pp interaction region, a large-area silicon-strip detector located upstream of a dipole magnet with a bending power of about 4 Tm, and three stations of silicon-strip detectors and straw drift tubes placed downstream. The combined tracking system has momentum resolution $\Delta p/p$ that varies from 0.4% at 5 GeV to 0.6% at 100 GeV, and impact parameter (IP) resolution of 20 μm for tracks with high transverse momentum (p_T).² Charged hadrons are identified using two ring-imaging Cherenkov detectors. Photon, electron and hadron candidates are identified by a calorimeter system consisting of scintillating-pad and preshower detectors, an electromagnetic calorimeter and a hadronic calorimeter. Muons are identified by a system composed of alternating layers of iron and multiwire proportional chambers. The trigger [19] consists of a hardware stage, based on information from the calorimeter and muon systems, followed by a software stage

¹The inclusion of charge-conjugate states is implied in this Letter.

²We use mass and momentum units in which $c = 1$.

which applies a full event reconstruction.

In the offline analysis $J/\psi \rightarrow \mu^+\mu^-$ candidates are selected with the following criteria: $p_T(\mu) > 0.9$ GeV, $p_T(J/\psi) > 1.5$ GeV, χ^2 per degree of freedom for the two muons to form a common vertex, $\chi_{\text{vtx}}^2(\mu^+\mu^-)/\text{ndf} < 9$, and a mass consistent with the J/ψ meson. The separation of the J/ψ decay vertex from the nearest primary vertex (PV) must be at least three standard deviations. Combinations of $K^+\pi^-\pi^+$ candidates that are consistent with originating from a common vertex with $\chi_{\text{vtx}}^2(K^+\pi^-\pi^+)/\text{ndf} < 9$, with each charged hadron (h) separated from all PVs ($\chi_{\text{IP}}^2(h) > 9$) and having $p_T(h) > 0.25$ GeV, are selected. The quantity $\chi_{\text{IP}}^2(h)$ is defined as the difference between the χ^2 of the PV reconstructed with and without the considered particle. Kaon and pion candidates are required to satisfy $\ln[\mathcal{L}(K)/\mathcal{L}(\pi)] > 0$ and < 5 , respectively, where \mathcal{L} is the particle identification likelihood [20]. If both same-sign hadrons in this combination meet the kaon requirement, only the particle with higher p_T is considered a kaon candidate. We combine J/ψ candidates with $K^+\pi^-\pi^+$ candidates to form B^+ candidates, which must satisfy $\chi_{\text{vtx}}^2(J/\psi K^+\pi^-\pi^+)/\text{ndf} < 9$, $p_T(B^+) > 2$ GeV and have decay time greater than 0.25 ps. The $J/\psi K^+\pi^-\pi^+$ mass is calculated using the known J/ψ mass and the B vertex as constraints.

Four discriminating variables (x_i) are used in a likelihood ratio to improve the background suppression: the minimal $\chi_{\text{IP}}^2(h)$, $\chi_{\text{vtx}}^2(J/\psi K^+\pi^-\pi^+)/\text{ndf}$, $\chi_{\text{IP}}^2(B^+)$, and the cosine of the largest opening angle between the J/ψ and the charged-hadron transverse momenta. The latter peaks at positive values for the signal as the B^+ meson has a high transverse momentum. Background events in which particles are combined from two different B decays peak at negative values, whilst those due to random combinations of particles are more uniformly distributed. The four 1D signal probability density functions (PDFs), $\mathcal{P}_{\text{sig}}(x_i)$, are obtained from a simulated sample of $B^+ \rightarrow \psi(2S)K^+$, $\psi(2S) \rightarrow \pi^+\pi^-J/\psi$ decays, which are kinematically similar to the signal decays. The data sample of $B^+ \rightarrow \psi(2S)K^+$ events is used as a control sample for $\mathcal{P}_{\text{sig}}(x_i)$ and for systematic studies in the angular analysis. The background PDFs, $\mathcal{P}_{\text{bkg}}(x_i)$, are obtained from the data in the B^+ mass sidebands (4.85–5.10 and 5.45–6.50 GeV). We require $-2 \sum_{i=1}^4 \ln[\mathcal{P}_{\text{sig}}(x_i)/\mathcal{P}_{\text{bkg}}(x_i)] < 1.0$, which preserves about 94% of the $X(3872)$ signal events.

About 38 000 candidates are selected in a $\pm 2\sigma$ mass range around the B^+ peak in the $M(J/\psi \pi^+\pi^- K^+)$ distribution, with a signal purity of 89%. The $\Delta M = M(\pi^+\pi^- J/\psi) - M(J/\psi)$ distribution is shown in Fig. 1. Fits to the $\psi(2S)$ and $X(3872)$ signals are shown in the insets. A Crystal Ball function [21] with symmetric tails is used for the signal shapes. The background is assumed to be linear. The $\psi(2S)$ fit is performed in the 539.2–639.2 MeV range leaving all parameters free to vary. It yields 5642 ± 76 signal (230 ± 21 background) candidates with a ΔM resolution of $\sigma_{\Delta M} = 3.99 \pm 0.05$ MeV, corresponding to a signal purity of 99.2% within a $\pm 2.5\sigma_{\Delta M}$ region. When fitting in the 723–823 MeV range, the signal tail parameters are fixed to the values obtained in the $\psi(2S)$ fit, which also describe well the simulated $X(3872)$ signal distribution. The fit yields 313 ± 26 $B^+ \rightarrow X(3872)K^+$ (568 ± 31 background) candidates with a resolution of 5.5 ± 0.5 MeV, corresponding to a signal purity of 68% within a $\pm 2.5\sigma_{\Delta M}$ region. The dominant source of background is from $B^+ \rightarrow J/\psi K_1(1270)^+$, $K_1(1270)^+ \rightarrow K^+\pi^+\pi^-$

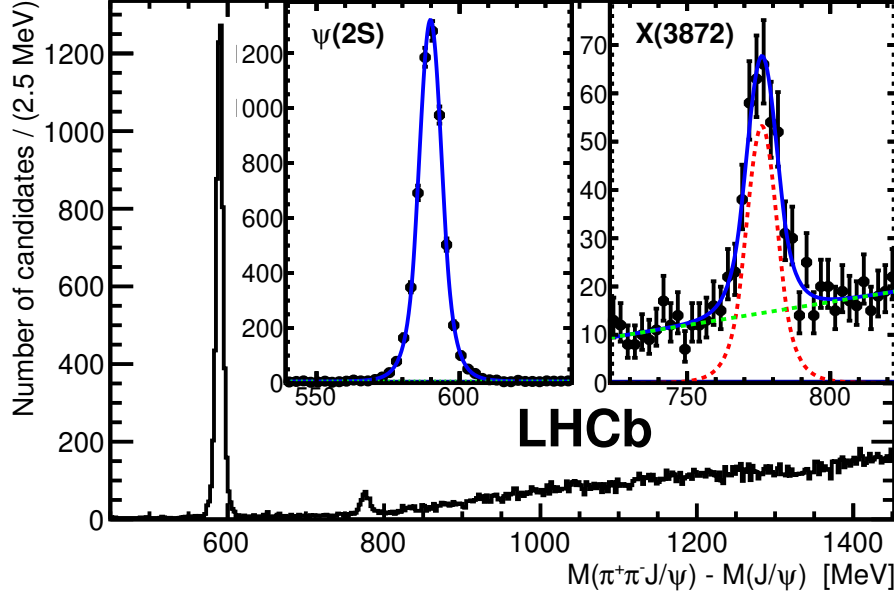


Figure 1: Distribution of ΔM for $B^+ \rightarrow J/\psi K^+ \pi^+ \pi^-$ candidates. The fits of the $\psi(2S)$ and $X(3872)$ signals are displayed. The solid blue, dashed red, and dotted green lines represent the total fit, signal component, and background component, respectively.

decays as found by studying the $K^+ \pi^+ \pi^-$ mass distribution.

The angular correlations in the B^+ decay carry information about the $X(3872)$ quantum numbers. To discriminate between the 1^{++} and 2^{-+} assignments we use the likelihood-ratio test, which in general provides the most powerful test between two hypotheses [22]. The PDF for each J^{PC} hypothesis, J_X , is defined in the 5D angular space $\Omega \equiv (\cos \theta_X, \cos \theta_{\pi\pi}, \Delta\phi_{X,\pi\pi}, \cos \theta_{J/\psi}, \Delta\phi_{X,J/\psi})$ by the normalized product of the expected decay matrix element (\mathcal{M}) squared and of the reconstruction efficiency (ϵ), $\mathcal{P}(\Omega|J_X) = |\mathcal{M}(\Omega|J_X)|^2 \epsilon(\Omega) / I(J_X)$, where $I(J_X) = \int |\mathcal{M}(\Omega|J_X)|^2 \epsilon(\Omega) d\Omega$. The efficiency is averaged over the $\pi^+ \pi^-$ mass ($M(\pi\pi)$) using a simulation [23–27] that assumes the $X(3872) \rightarrow \rho(770) J/\psi$, $\rho(770) \rightarrow \pi^+ \pi^-$ decay [6, 16, 28]. The observed $M(\pi\pi)$ distribution is in good agreement with this simulation. The lineshape of the $\rho(770)$ resonance can change slightly depending on the spin hypothesis. The effect on $\epsilon(\Omega)$ is found to be very small and is neglected. We follow the approach adopted in Ref. [12] to predict the matrix elements. The angular correlations are obtained using the helicity formalism,

$$|\mathcal{M}(\Omega|J_X)|^2 = \sum_{\Delta\lambda_\mu=-1,+1} \left| \sum_{\lambda_{J/\psi}, \lambda_{\pi\pi}=-1,0,+1} A_{\lambda_{J/\psi}, \lambda_{\pi\pi}} \times D_{0, \lambda_{J/\psi}-\lambda_{\pi\pi}}^{J_X}(\phi_X, \theta_X, -\phi_X) \times D_{\lambda_{\pi\pi}, 0}^1(\phi_{\pi\pi}, \theta_{\pi\pi}, -\phi_{\pi\pi}) \times D_{\lambda_{J/\psi}, \Delta\lambda_\mu}^1(\phi_{J/\psi}, \theta_{J/\psi}, -\phi_{J/\psi}) \right|^2,$$

where λ are particle helicities and $D_{\lambda_1, \lambda_2}^J$ are Wigner functions [13–15]. The helicity

couplings, $A_{\lambda_{J/\psi}, \lambda_{\pi\pi}}$, are expressed in terms of the LS couplings [29, 30], B_{LS} , where L is the orbital angular momentum between the $\pi\pi$ system and the J/ψ meson, and S is the sum of their spins. Since the energy release in the $X(3872) \rightarrow \rho(770)J/\psi$ decay is small, the lowest value of L is expected to dominate, especially because the next-to-minimal value is not allowed by parity conservation. The lowest value for the 1^{++} hypothesis is $L = 0$, which implies $S = 1$. With only one LS amplitude present, the angular distribution is completely determined without free parameters. For the 2^{-+} hypothesis the lowest value is $L = 1$, which implies $S = 1$ or 2 . As both LS combinations are possible, the 2^{-+} hypothesis implies two parameters, which are chosen to be the real and imaginary parts of $\alpha \equiv B_{11}/(B_{11} + B_{12})$. Since they are related to strong dynamics, they are difficult to predict theoretically and are treated as nuisance parameters.

We define a test statistic $t = -2 \ln[\mathcal{L}(2^{-+})/\mathcal{L}(1^{++})]$, where the $\mathcal{L}(2^{-+})$ likelihood is maximized with respect to α . The efficiency $\epsilon(\Omega)$ is not determined on an event-by-event basis, since it cancels in the likelihood ratio except for the normalization integrals. A large sample of simulated events, with uniform angular distributions, passed through a full simulation of the detection and the data selection process, is used to carry out the integration, $I(J_X) \propto \sum_{i=1}^{N_{\text{MC}}} |\mathcal{M}(\Omega_i|J_X)|^2$, where N_{MC} is the number of reconstructed simulated events. The background in the data is subtracted in the log-likelihoods using the *sPlot* technique [31] by assigning to each candidate in the fitted ΔM range an event weight (*sWeight*), w_i , based on its ΔM value, $-2 \ln \mathcal{L}(J_X) = -s_w 2 \sum_{i=1}^{N_{\text{data}}} w_i \ln \mathcal{P}(\Omega_i|J_X)$. Here, s_w is a constant scaling factor, $s_w = \sum_{i=1}^{N_{\text{data}}} w_i / \sum_{i=1}^{N_{\text{data}}} w_i^2$, which accounts for statistical fluctuations in the background subtraction. Positive (negative) values of the test statistic for the data, t_{data} , favor the 1^{++} (2^{-+}) hypothesis. The analysis procedure has been extensively tested on simulated samples for the 1^{++} and 2^{-+} hypotheses with different values of α , generated using the EVTGEN package [25].

The value of α that minimizes $-2 \ln \mathcal{L}(J_X = 2^{-+}, \alpha)$ in the data is $\hat{\alpha} = (0.671 \pm 0.046, 0.280 \pm 0.046)$. This is compatible with the value reported by Belle, $(0.64, 0.27)$ [16]. The value of the test statistic observed in the data is $t_{\text{data}} = +99$, thus favoring the 1^{++} hypothesis. Furthermore, $\hat{\alpha}$ is consistent with the value of α obtained from fitting a large background-free sample of simulated 1^{++} events, $(0.650 \pm 0.011, 0.294 \pm 0.012)$. The value of t_{data} is compared with the distribution of t in the simulated experiments to determine a p -value for the 2^{-+} hypothesis via the fraction of simulated experiments yielding a value of $t > t_{\text{data}}$. We simulate 2 million experiments with the value of α , and the number of signal and background events, as observed in the data. The background is assumed to be saturated by the $B^+ \rightarrow J/\psi K_1(1270)^+$ decay, which provides a good description of its angular correlations. None of the values of t from the simulated experiments even approach t_{data} , indicating a p -value smaller than $1/(2 \times 10^6)$, which corresponds to a rejection of the 2^{-+} hypothesis with greater than 5σ significance. As shown in Fig. 2, the distribution of t is reasonably well approximated by a Gaussian function. Based on the mean and r.m.s. spread of the t distribution for the 2^{-+} experiments, this hypothesis is rejected with a significance of 8.4σ . The deviations of the t distribution from the Gaussian function suggest this is a plausible estimate. Using phase-space $B^+ \rightarrow J/\psi K^+ \pi^+ \pi^-$ decays as a model for the background events, we obtain a consistent result. The value of t_{data}

falls into the region where the probability density for the 1^{++} simulated experiments is high. Integrating the 1^{++} distribution from $-\infty$ to t_{data} gives $\text{CL}(1^{++}) = 34\%$. We also compare the binned distribution of single-event log-likelihood-ratios with *sWeights* applied, $\ln[\mathcal{P}(\Omega_i|2^{-+}, \hat{\alpha})/\mathcal{P}(\Omega_i|1^{++})]$, between the data and the simulations. The shape of this distribution in data is consistent with the 1^{++} simulations and inconsistent with the 2^{-+} simulations, as illustrated in Fig. 3.

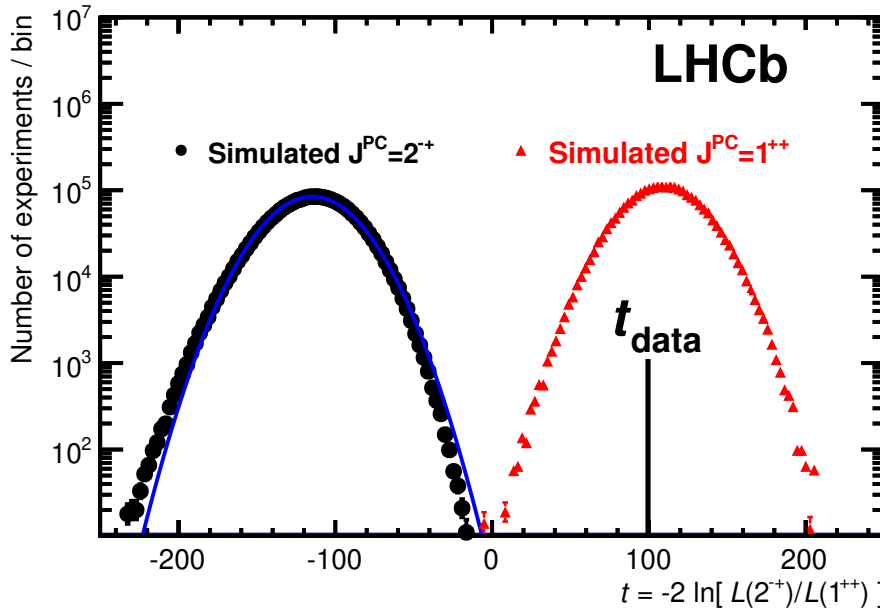


Figure 2: Distribution of the test statistic t for the simulated experiments with $J^{PC} = 2^{-+}$ and $\alpha = \hat{\alpha}$ (black circles on the left) and with $J^{PC} = 1^{++}$ (red triangles on the right). A Gaussian fit to the 2^{-+} distribution is overlaid (blue solid line). The value of the test statistic for the data, t_{data} , is shown by the solid vertical line.

We vary the data selection criteria to probe for possible biases from the background subtraction and the efficiency corrections. The nominal selection does not bias the $M(\pi\pi)$ distribution. By requiring $Q = M(J/\psi\pi\pi) - M(J/\psi) - M(\pi\pi) < 0.1$ GeV, we reduce the background level by a factor of four, while losing only 21% of the signal. The significance of the 2^{-+} rejection changes very little, in agreement with the simulations. By tightening the requirements on the p_T of π , K and μ candidates, we decrease the signal efficiency by about 50% with similar reduction in the background level. In all cases, the significance of the 2^{-+} rejection is reduced by a factor consistent with the simulations.

In the analysis we use simulations to calculate the $I(J_X)$ integrals. In an alternative approach to the efficiency estimates, we use the $B^+ \rightarrow \psi(2S)K^+$ events observed in the data weighted by the inverse of 1^{--} matrix element squared. We obtain a value of t_{data} that corresponds to 8.2σ rejection of the 2^{-+} hypothesis.

As an additional goodness-of-fit test for the 1^{++} hypothesis, we project the data onto five 1D and ten 2D binned distributions in all five angles and their combinations. They are all consistent with the distributions expected for the 1^{++} hypothesis. Some of them

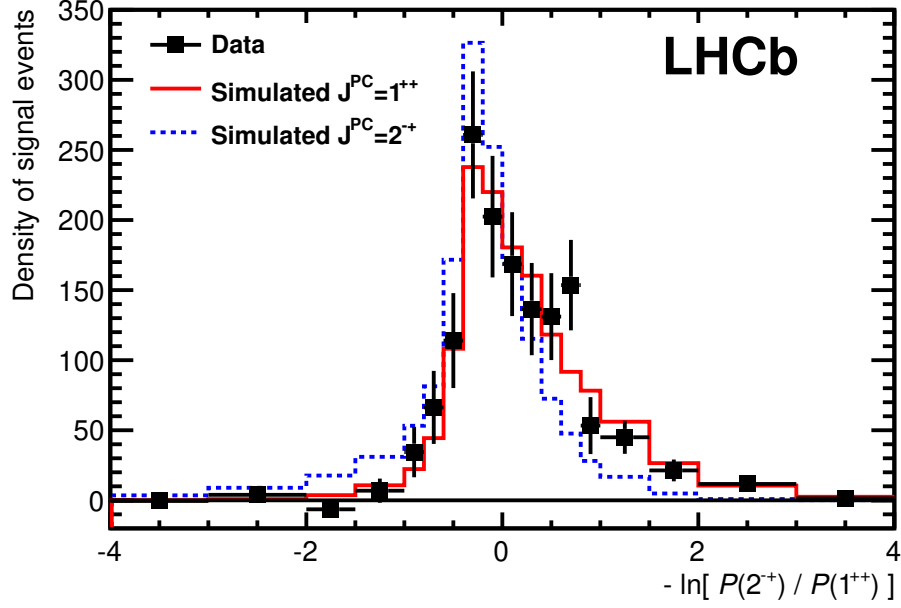


Figure 3: Distribution of $-\ln[\mathcal{P}(\Omega_i|2^{++}, \hat{\alpha})/\mathcal{P}(\Omega_i|1^{++})]$ for the data (points with error bars) compared to the distributions for the simulated experiments with $J^{PC} = 1^{++}$ (red solid histogram) and with $J^{PC} = 2^{++}$, $\alpha = \hat{\alpha}$ (blue dashed histogram) after the background subtraction using *sWeights*. The simulated distributions are normalized to the number of signal candidates observed in the data. Bin contents and uncertainties are divided by bin width because of unequal bin sizes.

are inconsistent with the distributions expected for the $(2^{++}, \hat{\alpha})$ hypothesis. The most significant inconsistency is observed for the 2D projections onto $\cos\theta_X$ vs. $\cos\theta_{\pi\pi}$. The separation between the 1^{++} and 2^{++} hypotheses increases when using correlations between these two angles, as illustrated in Fig. 4.

In summary, we unambiguously establish that the values of total angular momentum, parity and charge-conjugation eigenvalues of the $X(3872)$ state are 1^{++} . This is achieved through the first analysis of the full five-dimensional angular correlations between final state particles in $B^+ \rightarrow X(3872)K^+$, $X(3872) \rightarrow \pi^+\pi^-J/\psi$, $J/\psi \rightarrow \mu^+\mu^-$ decays using the likelihood-ratio test. The 2^{++} hypothesis is excluded with a significance of more than eight Gaussian standard deviations. This result rules out the explanation of the $X(3872)$ meson as a conventional $\eta_{c2}(1^1D_2)$ state. Among the remaining possibilities are the $\chi_{c1}(2^3P_1)$ charmonium, disfavored by the value of the $X(3872)$ mass [32], and unconventional explanations such as a $D^{*0}\bar{D}^0$ molecule [7], tetraquark state [8] or charmonium-molecule mixture [9].

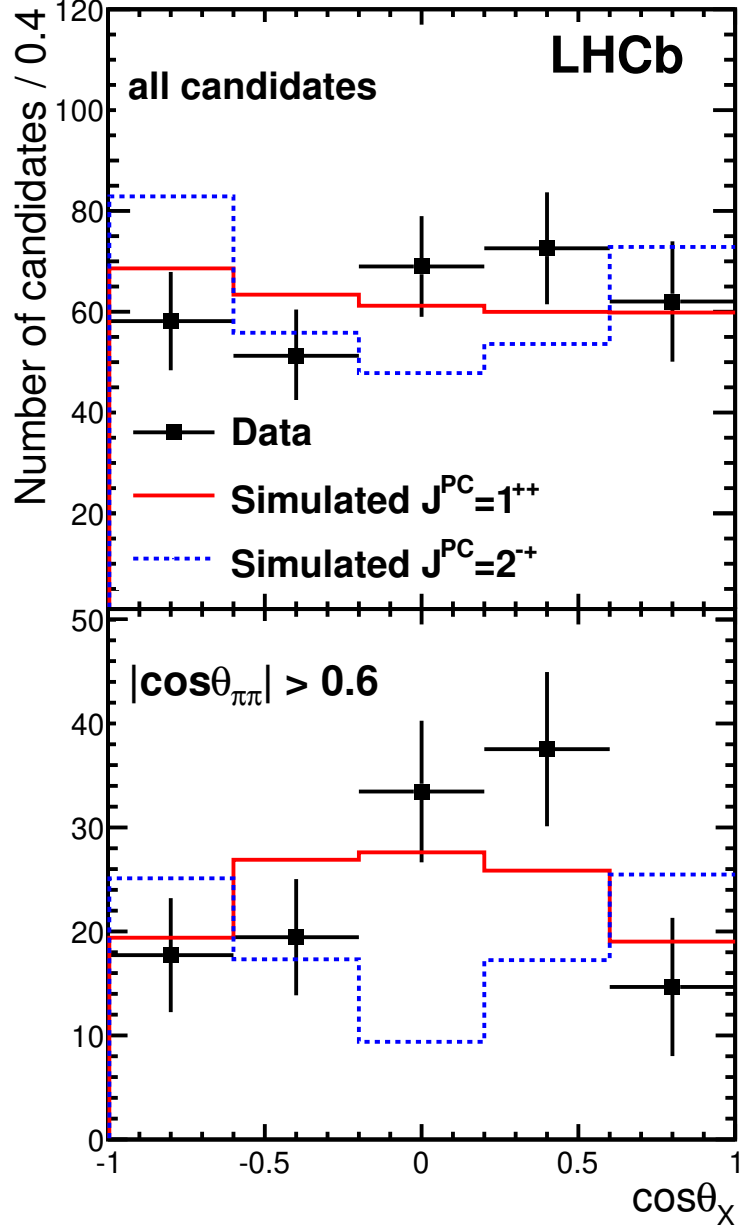


Figure 4: Background-subtracted distribution of $\cos \theta_X$ for (top) all candidates and for (bottom) candidates with $|\cos \theta_{\pi\pi}| > 0.6$ for the data (points with error bars) compared to the expected distributions for the $J^{PC} = 1^{++}$ (red solid histogram) and $J^{PC} = 2^{-+}$ and $\alpha = \hat{\alpha}$ hypotheses (blue dashed histogram). The simulated distributions are normalized to the number of signal candidates observed in the data across the full phase space.

Acknowledgements

We express our gratitude to our colleagues in the CERN accelerator departments for the excellent performance of the LHC. We thank the technical and administrative staff

at the LHCb institutes. We acknowledge support from CERN and from the national agencies: CAPES, CNPq, FAPERJ and FINEP (Brazil); NSFC (China); CNRS/IN2P3 and Region Auvergne (France); BMBF, DFG, HGF and MPG (Germany); SFI (Ireland); INFN (Italy); FOM and NWO (The Netherlands); SCSR (Poland); ANCS/IFA (Romania); MinES, Rosatom, RFBR and NRC “Kurchatov Institute” (Russia); MinECo, XuntaGal and GENCAT (Spain); SNSF and SER (Switzerland); NAS Ukraine (Ukraine); STFC (United Kingdom); NSF (USA). We also acknowledge the support received from the ERC under FP7. The Tier1 computing centres are supported by IN2P3 (France), KIT and BMBF (Germany), INFN (Italy), NWO and SURF (The Netherlands), PIC (Spain), GridPP (United Kingdom). We are thankful for the computing resources put at our disposal by Yandex LLC (Russia), as well as to the communities behind the multiple open source software packages that we depend on.

References

- [1] Belle collaboration, S.-K. Choi *et al.*, *Observation of a narrow charmonium-like state in exclusive $B^\pm \rightarrow K^\pm \pi^+ \pi^- J/\psi$ decays*, Phys. Rev. Lett. **91** (2003) 262001, [arXiv:hep-ex/0309032](#).
- [2] CDF collaboration, D. Acosta *et al.*, *Observation of the narrow state $X(3872) \rightarrow J/\psi \pi^+ \pi^-$ in $p\bar{p}$ collisions at $\sqrt{s} = 1.96$ TeV*, Phys. Rev. Lett. **93** (2004) 072001, [arXiv:hep-ex/0312021](#).
- [3] D0 collaboration, V. M. Abazov *et al.*, *Observation and properties of the $X(3872)$ decaying to $J/\psi \pi^+ \pi^-$ in $p\bar{p}$ collisions at $\sqrt{s} = 1.96$ TeV*, Phys. Rev. Lett. **93** (2004) 162002, [arXiv:hep-ex/0405004](#).
- [4] BaBar collaboration, B. Aubert *et al.*, *Study of the $B^- \rightarrow J/\psi K^- \pi^+ \pi^-$ decay and measurement of the $B^- \rightarrow X(3872) K^-$ branching fraction*, Phys. Rev. **D71** (2005) 071103, [arXiv:hep-ex/0406022](#).
- [5] LHCb collaboration, R. Aaij *et al.*, *Observation of $X(3872)$ production in pp collisions at $\sqrt{s} = 7$ TeV*, Eur. Phys. J. **C72** (2012) 1972, [arXiv:1112.5310](#).
- [6] CMS collaboration, S. Chatrchyan *et al.*, *Measurement of the $X(3872)$ production cross section via decays to $J/\psi \pi \pi$ in pp collisions at $\sqrt{s} = 7$ TeV*, [arXiv:1302.3968](#).
- [7] N. A. Tornqvist, *Isospin breaking of the narrow charmonium state of Belle at 3872-MeV as a deuson*, Phys. Lett. **B590** (2004) 209, [arXiv:hep-ph/0402237](#).
- [8] L. Maiani, F. Piccinini, A. D. Polosa, and V. Riquer, *Diquark-antidiquarks with hidden or open charm and the nature of $X(3872)$* , Phys. Rev. **D71** (2005) 014028, [arXiv:hep-ph/0412098](#).

- [9] C. Hanhart, Y. Kalashnikova, and A. Nefediev, *Interplay of quark and meson degrees of freedom in a near-threshold resonance: multi-channel case*, Eur. Phys. J. **A47** (2011) 101, [arXiv:1106.1185](#).
- [10] BaBar collaboration, B. Aubert *et al.*, *Search for $B^+ \rightarrow X(3872)K^+$, $X(3872) \rightarrow J/\psi\gamma$* , Phys. Rev. **D74** (2006) 071101, [arXiv:hep-ex/0607050](#).
- [11] Belle collaboration, V. Bhardwaj *et al.*, *Observation of $X(3872) \rightarrow J/\psi\gamma$ and search for $X(3872) \rightarrow \psi'\gamma$ in B decays*, Phys. Rev. Lett. **107** (2011) 091803, [arXiv:1105.0177](#).
- [12] CDF collaboration, A. Abulencia *et al.*, *Analysis of the quantum numbers J^{PC} of the $X(3872)$* , Phys. Rev. Lett. **98** (2007) 132002, [arXiv:hep-ex/0612053](#).
- [13] M. Jacob and G. Wick, *On the general theory of collisions for particles with spin*, Annals Phys. **7** (1959) 404.
- [14] J. D. Richman, *An experimenter's guide to the helicity formalism*, 1984, CALT-68-1148.
- [15] S. U. Chung, *General formulation of covariant helicity-coupling amplitudes*, Phys. Rev. **D57** (1998) 431.
- [16] Belle collaboration, S.-K. Choi *et al.*, *Bounds on the width, mass difference and other properties of $X(3872) \rightarrow \pi^+\pi^-J/\psi$ decays*, Phys. Rev. **D84** (2011) 052004, [arXiv:1107.0163](#).
- [17] BaBar collaboration, P. del Amo Sanchez *et al.*, *Evidence for the decay $X(3872) \rightarrow J/\psi\omega$* , Phys. Rev. **D82** (2010) 011101, [arXiv:1005.5190](#).
- [18] LHCb collaboration, A. A. Alves Jr. *et al.*, *The LHCb detector at the LHC*, JINST **3** (2008) S08005.
- [19] R. Aaij *et al.*, *The LHCb trigger and its performance*, [arXiv:1211.3055](#), submitted to JINST.
- [20] M. Adinolfi *et al.*, *Performance of the LHCb RICH detector at the LHC*, [arXiv:1211.6759](#).
- [21] T. Skwarnicki, *A study of the radiative cascade transitions between the Υ' and Υ resonances*, PhD thesis, Institute of Nuclear Physics, Krakow, 1986, DESY-F31-86-02.
- [22] F. James, *Statistical methods in experimental physics*, World Scientific Publishing, 2006.
- [23] T. Sjöstrand, S. Mrenna, and P. Skands, *PYTHIA 6.4 physics and manual*, JHEP **05** (2006) 026, [arXiv:hep-ph/0603175](#).

- [24] I. Belyaev *et al.*, *Handling of the generation of primary events in GAUSS, the LHCb simulation framework*, Nuclear Science Symposium Conference Record (NSS/MIC) **IEEE** (2010) 1155.
- [25] D. J. Lange, *The EvtGen particle decay simulation package*, Nucl. Instrum. Meth. **A462** (2001) 152.
- [26] GEANT4 collaboration, J. Allison *et al.*, *Geant4 developments and applications*, IEEE Trans. Nucl. Sci. **53** (2006) 270; GEANT4 collaboration, S. Agostinelli *et al.*, *GEANT4: a simulation toolkit*, Nucl. Instrum. Meth. **A506** (2003) 250.
- [27] M. Clemencic *et al.*, *The LHCb simulation application, GAUSS: design, evolution and experience*, J. of Phys. : Conf. Ser. **331** (2011) 032023.
- [28] CDF collaboration, A. Abulencia *et al.*, *Measurement of the dipion mass spectrum in $X(3872) \rightarrow J/\psi \pi^+ \pi^-$ decays.*, Phys. Rev. Lett. **96** (2006) 102002, [arXiv:hep-ex/0512074](#).
- [29] J. Heuser, *Measurement of the mass and the quantum numbers J^{PC} of the $X(3872)$ state*, PhD thesis, Universitat Karlsruhe, 2008, IEKP-KA/2008-16.
- [30] N. Mangiafave, *Measurements of charmonia production and a study of the $X(3872)$ at LHCb*, PhD thesis, Cambridge, 2012, CERN-THESIS-2012-003.
- [31] M. Pivk and F. R. Le Diberder, *sPlot: a statistical tool to unfold data distributions*, Nucl. Instrum. Meth. **A555** (2005) 356, [arXiv:physics/0402083v3](#).
- [32] T. Skwarnicki, *Heavy quarkonium*, Int. J. Mod. Phys. **A19** (2004) 1030, [arXiv:hep-ph/0311243](#).